

# The SABEMMT Aerodynamic and Structural Model for Propellers

Miguel Frade Saavedra

December 2025

© 2025 Miguel Frade Saavedra.

## 1. Introduction

SABEMMT (Structures And Blade Element Modified Momentum Theory) is a robust high-fidelity BEMT implementation for propeller analysis and design, integrating structural calculations and modified momentum theory. The model accounts for multi-regime simulation, considers the effects of Reynolds number at all sections of the blade and implements Prandtl tip loss function.

It is a general-purpose aerodynamic and structural model for the analysis and optimization of:

- Airplane propellers
- Helicopter rotors in axial flight
- Multirotor propellers in axial flight

The whole project can be found for free at: <https://github.com/miguel-frade/sabemmt>.

This project is licensed under the Creative Commons Attribution–NonCommercial 4.0 International License (CC BY-NC 4.0). You are free to use, modify, and redistribute this code for personal, academic, and research purposes, provided that proper attribution is given.

Commercial use of this project is strictly prohibited. Commercial use includes, but is not limited to, use in proprietary software, paid services, consulting, or products sold for profit.

If you use, adapt, or build upon the results, methods, or proofs presented in this document, you are requested to cite this work as:

*Miguel Frade Saavedra, “The SABEMMT Aerodynamic and Structural Model for Propellers,” December 2025. Available at: <https://github.com/miguel-frade/sabemmt>*

## 2. Aerodynamic model

The aerodynamic model is based on BEMT (Blade Element Momentum Theory), which combines Blade Element Theory with Momentum Theory. However, SABEMMT implements an Engineering Modification of the classical Momentum Theory, as proposed in Cuerva Tejero, Sanz Andrés, et al. (2006). It is important to mention that all BEMT models assume that no fluid dynamic interaction occurs between different sections of the blade. Each blade element is affected only by the flow corresponding to its  $dr$ . Nevertheless, tip losses will be modeled using the Prandtl tip loss function.

## 2.1. Fundamentals of Blade Element Theory (BET) applied to rotors and propellers

The mathematical formulation of Blade Element Theory (BET) for the analysis of aerodynamic loads on propellers and rotors is detailed below. The kinematics of the airfoil sections, the decomposition of aerodynamic forces, and the non-dimensionalization of the equations to obtain the differentials of the thrust coefficient ( $dc_T$ ) and torque coefficient ( $dc_Q$ ) are described. The development concludes with the demonstration of the specific equations governing the local behavior of the blade element as a function of solidity and advance ratio.

### 2.1.1 Introduction

Blade Element Theory (BET) is a fundamental approach in aeronautical engineering for predicting the performance of propellers, helicopter rotors, and wind turbines. The central premise consists of discretizing the blade into a finite number of independent radial elements of differential width  $dr$ . It is assumed that each element acts as a two-dimensional (2D) airfoil subjected to a local velocity field, ignoring, as a first approximation, the interaction between adjacent elements (cross-flow).

### 2.1.2 Kinematics and velocities diagram

For a blade element located at a radial distance  $r$  from the axis of rotation, the relative flow field is the result of the combination of the rotational velocity and the axial flow velocity.

Let  $\Omega$  be the angular velocity of the rotor and  $V$  be the freestream velocity (or climb/forward speed). Additionally, the rotor induces a flow velocity  $v_i$  through the disc. The velocity components are defined as:

- **Tangential velocity ( $v_t$ ):** Due to the rotation of the disc.

$$v_t = \Omega r \quad (1)$$

- **Perpendicular velocity ( $v_n$ ):** Due to the axial motion and the induced velocity.

$$v_n = V + v_i \quad (2)$$

The resultant velocity  $v_R$  perceived by the airfoil is the vector sum of these components:

$$v_R = \sqrt{v_t^2 + v_n^2} \quad (3)$$

The relative flow angle  $\phi$  (angle of incidence of the flow with respect to the plane of rotation) is defined geometrically as:

$$\phi = \arctan\left(\frac{v_n}{v_t}\right) \quad (4)$$

### 2.1.3 Local aerodynamic forces

The fundamental aerodynamic forces act on the blade element: Lift ( $dL$ ), perpendicular to  $v_R$ , and Drag ( $dD$ ), parallel to  $v_R$ . Letting  $c$  be the local chord of the airfoil and  $\rho$  the air density:

$$dL = \frac{1}{2} \rho v_R^2 c \cdot c_l \cdot dr \quad (5)$$

$$dD = \frac{1}{2} \rho v_R^2 c \cdot c_d \cdot dr \quad (6)$$

Where  $c_l$  and  $c_d$  are the airfoil lift and drag coefficients, respectively, which depend on the effective angle of attack  $\alpha = \theta - \phi$  (where  $\theta$  is the geometric pitch) and also on the Reynolds number,  $Re$ .

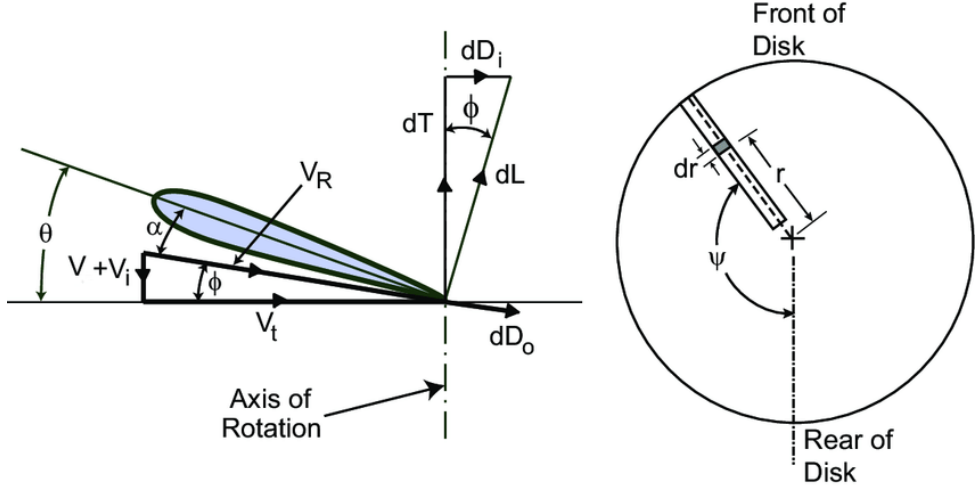


Figure 1: Diagram of velocities and aerodynamic forces on a blade element. Lift ( $dL$ ) and Drag ( $dD$ ) forces are shown projected onto the Thrust ( $dT$ ) and Torque ( $dQ$ ) axes. Author: Matt Garratt

#### 2.1.4 Force decomposition

From an engineering perspective, the forces projected onto the rotor axes are of interest:

1. **Thrust force ( $dT$ ):** Perpendicular to the plane of rotation (contributes to the total lift of the vehicle or thrust).
2. **In-plane resistance force or Torque force ( $dF_Q$ ):** Parallel to the plane of rotation (generates the required torque).

Projecting  $dL$  and  $dD$  using the angle  $\phi$ :

$$dT = dL \cos \phi - dD \sin \phi \quad (7)$$

$$dF_Q = dL \sin \phi + dD \cos \phi \quad (8)$$

The differential torque ( $dQ$ ) is the product of the tangential force and the lever arm  $r$ :

$$dQ = r \cdot (dL \sin \phi + dD \cos \phi) \quad (9)$$

#### 2.1.5 Non-dimensionalization

To arrive at the target formulas, we must introduce standard non-dimensional parameters in rotor theory. We define the non-dimensional radial position  $x$ , the advance ratio  $\mu$ , and the induced inflow ratio  $\lambda$ :

$$x = \frac{r}{R}, \quad (10)$$

$$\mu = \frac{V}{\Omega R}, \quad (11)$$

$$\lambda = \frac{v_i}{\Omega R} \quad (12)$$

Substituting these definitions into the resultant velocity equation  $v_R^2$ :

$$v_R^2 = (\Omega r)^2 + (V + v_i)^2 = (\Omega R)^2 [x^2 + (\mu + \lambda)^2] \quad (13)$$

### 2.1.6 Definition of Solidity ( $\sigma$ )

Rotor solidity ( $\sigma$ ) represents the ratio between the blade area and the disc area. For a rotor with  $N_b$  blades of chord  $c$ :

$$\sigma = \frac{N_b c}{\pi R} \Rightarrow N_b c = \sigma \pi R \quad (14)$$

### 2.1.7 Derivation of the Thrust Coefficient ( $dc_T$ )

The thrust coefficient is defined by normalizing the force by the disc area ( $A = \pi R^2$ ) and the blade tip dynamic pressure  $\rho(\Omega R)^2$ . For  $N_b$  blades:

$$dc_T = \frac{N_b \cdot dT}{\rho(\pi R^2)(\Omega R)^2} \quad (15)$$

Substituting  $dT$  (Eq. 6) and using the expressions for  $dL$  and  $dD$ :

$$dT = \frac{1}{2} \rho v_R^2 c \cdot (c_l \cos \phi - c_d \sin \phi) dr \quad (16)$$

Inserting this into the definition of  $dc_T$ :

$$dc_T = \frac{N_b [\frac{1}{2} \rho(\Omega R)^2 [x^2 + (\mu + \lambda)^2] c (c_l \cos \phi - c_d \sin \phi) dr]}{\rho \pi R^2 (\Omega R)^2} \quad (17)$$

Simplifying terms ( $\rho$  and  $(\Omega R)^2$  cancel out) and grouping  $\frac{N_b c}{\pi R}$  as  $\sigma$ :

$$dc_T = \frac{1}{2} \underbrace{\left( \frac{N_b c}{\pi R} \right)}_{\sigma} [x^2 + (\mu + \lambda)^2] (c_l \cos \phi - c_d \sin \phi) \frac{dr}{R} \quad (18)$$

Given that  $x = r/R$ , then  $dx = dr/R$ . We finally obtain:

$$dc_T = \frac{1}{2} \sigma [x^2 + (\mu + \lambda)^2] (c_l \cos \phi - c_d \sin \phi) \cdot dx \quad (19)$$

### 2.1.8 Derivation of the Torque Coefficient ( $dc_Q$ )

Analogously, the torque coefficient is normalized by including the radius  $R$  additionally in the denominator to non-dimensionalize the moment:

$$dc_Q = \frac{N_b \cdot dQ}{\rho(\pi R^2)(\Omega R)^2 R} \quad (20)$$

Recalling that  $dQ = r \cdot dF_Q$ :

$$dc_Q = \frac{N_b \cdot r \cdot \frac{1}{2} \rho v_R^2 c (c_l \sin \phi + c_d \cos \phi) dr}{\rho \pi R^3 (\Omega R)^2} \quad (21)$$

Replacing  $v_R^2$  and regrouping terms:

$$dc_Q = \frac{1}{2} \underbrace{\left( \frac{N_b c}{\pi R} \right)}_{\sigma} [x^2 + (\mu + \lambda)^2] (c_l \sin \phi + c_d \cos \phi) \underbrace{\frac{r}{R}}_x \underbrace{\frac{dr}{R}}_{dx} \quad (22)$$

Which results in the final formula:

$$dc_Q = \frac{1}{2} \sigma [x^2 + (\mu + \lambda)^2] (c_l \sin \phi + c_d \cos \phi) \cdot x \cdot dx \quad (23)$$

Finally, it is worth mentioning that lift and drag coefficients will be interpolated from experimental data, taking into account the effect of the Reynolds number:

$$c_l = c_l(\alpha, Re), \quad c_d = c_d(\alpha, Re).$$

## 2.2. Momentum Theory in the differential annulus

To complement the kinematic analysis of the blade, Momentum Theory is applied over an annular control volume. Unlike the global actuator disc approach, here it is considered that the flow through the rotor consists of a series of independent annular streamtubes of radius  $r$  and differential thickness  $dr$ , which do not interact with each other (radial independence hypothesis).

In this model, the blade element sweeps an annulus of area  $dA = 2\pi r dr$ . It is assumed that the rotor induces a pressure jump and a change in fluid momentum when crossing this differential disc.

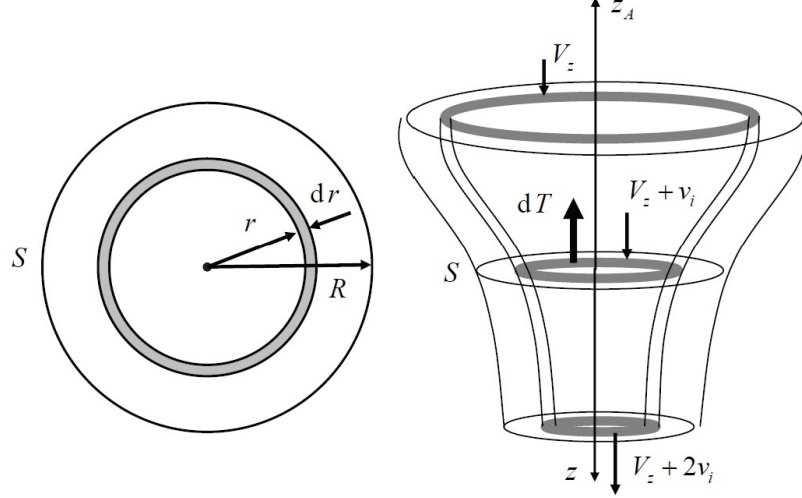


Figure 2: Differential control volume applied to an annulus of radius  $r$ . The streamtube and velocities upstream ( $V$ ), at the disc ( $V + v_i$ ), and in the far wake ( $V_{wake}$ ) are observed. Source: Cuerva Tejero, Espino Granado, et al. (2012).

Applying the principles of conservation of mass and momentum over this control volume, we analyze the mass flow rate  $d\dot{m}$  passing through the annular section. The axial velocity at the disc level is the sum of the freestream velocity  $V$  and the induced velocity  $v_i$ :

$$d\dot{m} = \rho \cdot dA \cdot (V + v_i) = \rho(2\pi r dr)(V + v_i) \quad (24)$$

According to the Froude-Rankine theorem, the velocity in the far wake ( $V_{wake}$ ) is  $V + 2v_i$ . The differential thrust  $dT$  generated by this annulus is equal to the rate of change of the fluid's axial momentum between upstream infinity and the far wake:

$$dT = d\dot{m} \cdot (V_{wake} - V) = [\rho(2\pi r dr)(V + v_i)] \cdot [(V + 2v_i) - V] \quad (25)$$

Simplifying the expression, we obtain the thrust equation based on momentum for the differential element:

$$dT = 4\pi\rho r(V + v_i)v_i \cdot dr \quad (26)$$

For this study, this classical equation is not used, because it is only valid for flight where  $(V + v_i) > 0$ . In order to subject the model to an optimization algorithm, we need a more robust equation that is valid for any flight condition. This will be the equation of the Modified Momentum Model, discussed below.

## 2.3. Modified Momentum Theory proposed in Cuerva Tejero, Sanz Andrés, et al. (2006)

Based on the formulation proposed in Cuerva Tejero, Sanz Andrés, et al. (2006), the differential thrust  $dT(r)$  considering corrections for vortex ring states and model continuity is expressed as:

$$dT(r) = 2\rho(2\pi r dr) [B^2 V^2 + (V + v_i)^2]^{1/2} Av_i \quad (27)$$

where:

- $V$  is the climb speed of the helicopter (or cruise speed of the airplane).
- $v_i$  is the induced velocity.
- $A$  and  $B$  are parameters of the model. The following values are taken:  $A = 0.745$  and  $B = 0.447$

**Non-dimensionalization of  $dc_T$ :** To obtain the differential thrust coefficient, we normalize the force by  $\rho(\pi R^2)(\Omega R)^2$ :

$$dc_T = \frac{dT}{\rho\pi R^2(\Omega R)^2} \quad (28)$$

Introducing standard non-dimensional variables:

$$x = \frac{r}{R}, \quad (29)$$

$$dx = \frac{dr}{R}, \quad (30)$$

$$\mu = \frac{V}{\Omega R}, \quad (31)$$

$$\lambda_i = \frac{v_i}{\Omega R} \quad (32)$$

Substituting equation (27) into (28):

$$dc_T = \frac{2\rho(2\pi x R \cdot R dx) [B^2(\mu\Omega R)^2 + (\mu\Omega R + \lambda\Omega R)^2]^{1/2} A(\lambda\Omega R)}{\rho\pi R^2(\Omega R)^2} \quad (33)$$

Factoring out the velocity terms  $\Omega R$  and simplifying the radius  $R$  and density  $\rho$ :

$$dc_T = \frac{4\pi\rho R^2 x dx \cdot (\Omega R) [B^2\mu^2 + (\mu + \lambda)^2]^{1/2} A\lambda(\Omega R)}{\rho\pi R^2(\Omega R)^2} \quad (34)$$

Cancelling common terms ( $\rho, \pi, R^2, (\Omega R)^2$ ), we obtain the final non-dimensional expression for Cuerva's model:

$$dc_T = 4A\lambda x \sqrt{B^2\mu^2 + (\mu + \lambda)^2} \cdot dx \quad (35)$$

## 2.4. Combination of BET and MMT considering the Prandtl Correction Factor to obtain an implicit expression to calculate $\lambda$

To obtain a more realistic solution that accounts for three-dimensional effects at the blade tips, the Prandtl Tip Loss Factor, denoted as  $F$ , is introduced. This factor corrects the overestimation of thrust near the blade tip ( $x = 1$ ) assuming that the wake vortex is a rigid helical sheet.

The correction factor  $F$  is defined as:

$$F = \frac{2}{\pi} \arccos \left( \exp \left[ -\frac{N_b(1-x)}{2|\sin \phi|} \right] \right) \quad (36)$$

Where  $N_b$  is the number of blades and  $\phi$  is the local relative flow angle. The value of  $F$  ranges between 0 (at the tip) and 1 (towards the root).

#### 2.4.1 Implicit equation for $\lambda$

To determine the operating point of each blade section, equilibrium must be satisfied between the aerodynamic forces generated by the airfoil (BET) and the change in fluid momentum (MMT).

Applying the factor  $F$  to the Modified Momentum equation, the corrected differential thrust coefficient becomes:

$$dc_{T,MMT} = F \cdot \left[ 4A\lambda x \sqrt{B^2\mu^2 + (\mu + \lambda)^2} \right] \cdot dx \quad (37)$$

Equating this expression with that obtained via Blade Element Theory (BET):

$$F \cdot 4A\lambda x \sqrt{B^2\mu^2 + (\mu + \lambda)^2} = \frac{1}{2}\sigma [x^2 + (\mu + \lambda)^2] (c_l \cos \phi - c_d \sin \phi) \quad (38)$$

This equality constitutes the implicit equation fundamental to the iterative method. Since  $F$ ,  $\phi$ ,  $c_l$ , and  $c_d$  are functions dependent on the induced velocity  $\lambda$ , the equation can be rewritten as a residual function  $f(\lambda) = 0$  for each radial position  $x$ :

$$\underbrace{F(\lambda) \cdot 4A\lambda x \sqrt{B^2\mu^2 + (\mu + \lambda)^2}}_{\text{Momentum (Corrected)}} - \underbrace{\frac{1}{2}\sigma [x^2 + (\mu + \lambda)^2] (c_l(\alpha) \cos \phi - c_d(\alpha) \sin \phi)}_{\text{Blade Element}} = 0 \quad (39)$$

To solve this equation, an iterative process (e.g., Newton-Raphson method) is required at each radial station  $x$ , recalling that:

$$\phi = \arctan \left( \frac{\mu + \lambda}{x} \right) \text{ and} \quad (40)$$

$$\alpha = \theta - \phi \quad (41)$$

#### 2.5. Calculation of global coefficients

Once the implicit system is resolved to determine the induced velocity distribution  $\lambda(x)$  and the local loads at each section are known, the propeller's global thrust ( $C_T$ ) and torque ( $C_Q$ ) coefficients are obtained by integrating the differentials radially from the root ( $x_h = R_{hub}/R$ ) to the blade tip ( $x = 1$ ).

$$C_T = \int_{x_0}^1 dc_T \quad (42)$$

$$C_Q = \int_{x_0}^1 dc_Q \quad (43)$$

Substituting the differential expressions obtained via Blade Element Theory, the definite integrals governing the global behavior of the propulsor are:

$$C_T = \int_{x_0}^1 \frac{1}{2}\sigma [x^2 + (\mu + \lambda)^2] (c_l \cos \phi - c_d \sin \phi) dx \quad (44)$$

$$C_Q = \int_{x_0}^1 \frac{1}{2}\sigma [x^2 + (\mu + \lambda)^2] (c_l \sin \phi + c_d \cos \phi) x dx \quad (45)$$

These integrals are usually solved numerically (using Riemann sums or the trapezoidal rule) by discretizing the blade into  $N$  elements, once the iterative process has converged for the value of  $\lambda$  at each station  $x$ .

#### 2.6. Total Forces, Power, and Efficiency

Once the global coefficients  $C_T$  and  $C_Q$  are obtained via integration, the physical dimensional magnitudes can be recovered by undoing the normalization applied previously.

The **Total Thrust Force** ( $T$ ) and **Total Torque** ( $Q$ ) are calculated as:

$$T = C_T \cdot \rho(\pi R^2)(\Omega R)^2 \quad (46)$$

$$Q = C_Q \cdot \rho(\pi R^3)(\Omega R)^2 \quad (47)$$

The **Power Required** ( $P$ ) to drive the propeller is obtained from the torque and angular velocity:

$$P = Q \cdot \Omega \quad (48)$$

Finally, the **Propulsive Efficiency** ( $\eta_p$ ) is defined as the ratio between useful power (power delivered to the fluid for propulsion) and brake power (power supplied to the shaft).

$$\eta_p = \frac{P_{\text{useful}}}{P_{\text{supplied}}} = \frac{T \cdot V}{P} = \frac{T \cdot V}{Q \cdot \Omega} \quad (49)$$

Substituting the expressions for  $T$  and  $Q$  as functions of their non-dimensional coefficients, and recalling that the advance ratio is  $\mu = V/(\Omega R)$ , the efficiency simplifies to:

$$\eta_p = \frac{C_T \cdot \rho \pi R^2 (\Omega R)^2 \cdot V}{C_Q \cdot \rho \pi R^3 (\Omega R)^2 \cdot \Omega} = \frac{C_T}{C_Q} \cdot \frac{V}{\Omega R} \quad (50)$$

Which results in the final expression dependent on the calculated coefficients and the flight condition:

$$\eta_p = \frac{C_T}{C_Q} \mu \quad (51)$$

However, a distinct limitation arises in the case of a helicopter in **hover**. In this flight condition, the forward velocity is zero ( $V = 0$ ), and consequently, the advance ratio is zero ( $\mu = 0$ ). According to Equation (6), this results in a propulsive efficiency of zero:

$$\eta_p = 0 \quad (52)$$

This is physically misleading for a helicopter, as the rotor is still expending significant energy to generate thrust and sustain the aircraft's weight, despite no useful work being done on the aircraft in the kinematic sense (force  $\times$  displacement).

To evaluate efficiency in static thrust conditions (hover), the **Figure of Merit** ( $FM$ ) is used. The Figure of Merit is defined as the ratio of the minimum ideal power required to generate a given thrust (derived from Momentum Theory) to the actual power supplied to the rotor:

$$FM = \frac{P_{\text{ideal}}}{P_{\text{actual}}} \quad (53)$$

From Momentum Theory, the ideal induced power ( $P_{\text{ideal}}$ ) required to generate a thrust  $T$  is:

$$P_{\text{ideal}} = \frac{T^{3/2}}{\sqrt{2\rho A}} \quad (54)$$

By substituting the expressions for Thrust ( $T$ ) and Power ( $P = Q \cdot \Omega$ ) using the non-dimensional coefficients  $C_T$  and  $C_Q$ , the expression becomes:

$$FM = \frac{(C_T \cdot \rho A (\Omega R)^2)^{3/2}}{\sqrt{2\rho A} \cdot (C_Q \cdot \rho A (\Omega R)^3)} \quad (55)$$

Simplifying the density ( $\rho$ ), area ( $A$ ), and tip speed ( $\Omega R$ ) terms, the standard non-dimensional form for the Figure of Merit is obtained:

$$FM = \frac{C_T^{3/2}}{\sqrt{2} C_Q} \quad (56)$$

This metric provides a measure of rotor efficiency in hover, where a value of  $FM = 1$  would indicate an ideal rotor with no profile drag or swirl losses (typically, real helicopters achieve an  $FM$  between 0.70 and 0.80).

## 2.7. Standard definitions for airplane propeller coefficients

In the fixed-wing aviation industry, it is standard convention to define aerodynamic coefficients as a function of revolutions per second ( $n$ ) and propeller diameter ( $D$ ), instead of angular velocity ( $\Omega$ ) and radius ( $R$ ) used in rotor and helicopter theory.

Defining the rotational frequency as  $n = \frac{\Omega}{2\pi}$  and diameter as  $D = 2R$ , standard coefficients are defined as (see McCormick (1979)):

$$C_{T_{std}} = \frac{T}{\rho n^2 D^4} \quad (57)$$

$$C_{Q_{std}} = \frac{Q}{\rho n^2 D^5} \quad (58)$$

$$C_{P_{std}} = \frac{P}{\rho n^3 D^5} \quad (59)$$

### 2.7.1 Coefficient conversion justification

The relationship between the coefficients derived in the previous section (denoted here as  $C_T$  and  $C_Q$ ) and standard coefficients is demonstrated below.

Thrust Coefficient ( $C_{T_{std}}$ ): Starting from the definition obtained via BET:

$$C_T = \frac{T}{\rho(\pi R^2)(\Omega R)^2} = \frac{T}{\rho\pi\Omega^2 R^4} \quad (60)$$

Substituting  $R = D/2$  and  $\Omega = 2\pi n$ :

$$C_T = \frac{T}{\rho\pi(2\pi n)^2(D/2)^4} = \frac{T}{\rho\pi(4\pi^2 n^2)(\frac{D^4}{16})} = \frac{T}{\rho n^2 D^4} \left( \frac{16}{\pi \cdot 4\pi^2} \right) \quad (61)$$

We recognize the term  $\frac{T}{\rho n^2 D^4}$  as  $C_{T_{std}}$ . Solving for  $C_{T_{std}}$  in terms of  $C_T$ :

$$C_T = C_{T_{std}} \frac{4}{\pi^3} \quad \Rightarrow \quad \boxed{C_{T_{std}} = C_T \cdot \frac{\pi^3}{4}} \quad (62)$$

Torque Coefficient ( $C_{Q_{std}}$ ): Analogously for torque, starting from the rotor definition:

$$C_Q = \frac{Q}{\rho(\pi R^2)(\Omega R)^2 R} = \frac{Q}{\rho\pi\Omega^2 R^5} \quad (63)$$

Substituting again  $R = D/2$  and  $\Omega = 2\pi n$ :

$$C_Q = \frac{Q}{\rho\pi(4\pi^2 n^2)(\frac{D^5}{32})} = \frac{Q}{\rho n^2 D^5} \left( \frac{32}{4\pi^3} \right) = C_{Q_{std}} \frac{8}{\pi^3} \quad (64)$$

Therefore, the direct conversion is:

$$\boxed{C_{Q_{std}} = C_Q \cdot \frac{\pi^3}{8}} \quad (65)$$

Power Coefficient ( $C_{P_{std}}$ ): The power absorbed by the propeller relates to torque via  $P = Q \cdot \Omega = Q \cdot 2\pi n$ . Substituting this into the standard power coefficient definition:

$$C_{P_{std}} = \frac{P}{\rho n^3 D^5} = \frac{Q \cdot 2\pi n}{\rho n^3 D^5} = 2\pi \left( \frac{Q}{\rho n^2 D^5} \right) \quad (66)$$

Since the term in parentheses is exactly  $C_{Q_{std}}$ , the simple relationship is obtained:

$$\boxed{C_{P_{std}} = 2\pi \cdot C_{Q_{std}}} \quad (67)$$

This justifies the use of simplified formulas in engineering calculation codes to transition between rotor theory notation and standard propeller notation.

### 3. Structural model

The functions involved in the structural calculation process for each blade are described below. For this, two major loading effects on the blade are assumed: those generated by centrifugal stresses, caused by centrifugal forces, and those generated by bending stresses, caused by aerodynamic forces.

In the structural analysis model, stresses are evaluated using the exact geometry of the airfoil cross-section in conjunction with the equations of classical beam theory. To account for the effects of blade geometric torsion, an appropriate rotation of forces and moments is required.

**Note:** In this section, the coordinates  $x$  and  $y$  are used to describe the geometry of each section, while the radial position along the blade is denoted by  $r$ . This notation should not be confused with that adopted in the aerodynamic analysis, where  $x$  represented the non-dimensional radial coordinate, defined as  $x = r/R$ .

#### 3.1. Geometric properties of the airfoil (blade section)

The airfoil geometry is defined by an upper surface  $y_u(x)$  and a lower surface  $y_l(x)$ , extending from the leading edge ( $x = 0$ ) to the trailing edge ( $x = c$ ).

The geometric properties are computed by integrating the thickness along the chord. The total cross-sectional area is:

$$A = \int_0^c (y_u(x) - y_l(x)) dx \quad (68)$$

The neutral axis (centroid) is not necessarily located at the geometric center. The coordinates of the centroid  $(x_c, y_c)$  are:

$$x_c = \frac{1}{A} \int_0^c x \cdot (y_u(x) - y_l(x)) dx \quad (69)$$

$$y_c = \frac{1}{A} \int_0^c \frac{1}{2}(y_u(x)^2 - y_l(x)^2) dx \quad (70)$$

To calculate the bending stiffness, we first compute the area moments of inertia with respect to the root coordinate system (where the Leading Edge is at 0,0):

$$I_{x,0} = \int_A y^2 dA = \frac{1}{3} \int_0^c (y_u(x)^3 - y_l(x)^3) dx \quad (71)$$

$$I_{y,0} = \int_A x^2 dA = \int_0^c x^2 (y_u(x) - y_l(x)) dx \quad (72)$$

These must be shifted to the centroidal axes to represent the beam's resistance to bending. Using the Parallel Axis Theorem:

$$I_x = I_{x,0} - A \cdot y_c^2 \quad (73)$$

$$I_y = I_{y,0} - A \cdot x_c^2 \quad (74)$$

##### 3.1.1 Normalized Airfoil Properties

To maintain computational efficiency, we define a normalized airfoil with chord  $c = 1$  using dimensionless coordinates  $\xi = x/c$  and  $\eta = y/c$ , where  $\xi \in [0, 1]$ .

The normalized area is defined as:

$$A_{\text{norm}} := \int_0^1 (\eta_u(\xi) - \eta_l(\xi)) d\xi \quad (75)$$

The normalized centroid location is:

$$\xi_c = \frac{1}{A_{\text{norm}}} \int_0^1 \xi(\eta_u - \eta_l) d\xi \quad , \quad \eta_c = \frac{1}{A_{\text{norm}}} \int_0^1 \frac{1}{2}(\eta_u^2 - \eta_l^2) d\xi \quad (76)$$

And the normalized area moments of inertia (about the centroid) are:

$$I_{x,\text{norm}} := \underbrace{\left[ \frac{1}{3} \int_0^1 (\eta_u^3 - \eta_l^3) d\xi \right]}_{I_{x,0,\text{norm}}} - A_{\text{norm}} \cdot \eta_c^2 \quad (77)$$

$$I_{y,\text{norm}} := \underbrace{\left[ \int_0^1 \xi^2(\eta_u - \eta_l) d\xi \right]}_{I_{y,0,\text{norm}}} - A_{\text{norm}} \cdot \xi_c^2 \quad (78)$$

### 3.1.2 Scaling to real chord

Once the normalized properties ( $A_{\text{norm}}$ ,  $I_{x,\text{norm}}$ ,  $I_{y,\text{norm}}$ ) are computed for the specific airfoil shape, they can be scaled to any section of chord  $c$  using the following relationships:

$$A = c^2 \cdot A_{\text{norm}} \quad (79)$$

$$I_x = c^4 \cdot I_{x,\text{norm}} \quad (80)$$

$$I_y = c^4 \cdot I_{y,\text{norm}} \quad (81)$$

Additionally, the physical location of the centroid scales linearly:

$$x_c = c \cdot \xi_c \quad , \quad y_c = c \cdot \eta_c \quad (82)$$

### 3.1.3 Product of Inertia

Real airfoils are generally asymmetric, meaning the standard chordwise ( $x$ ) and flapwise ( $y$ ) axes are not the principal axes of bending. To capture the coupling between flapwise and edgewise bending, we must calculate the Product of Inertia,  $I_{xy}$ .

The product of inertia with respect to the root coordinate system is:

$$I_{xy,0} = \int_A xy dA = \int_0^c x \left[ \int_{y_l(x)}^{y_u(x)} y dy \right] dx = \frac{1}{2} \int_0^c x(y_u(x)^2 - y_l(x)^2) dx \quad (83)$$

Using the Parallel Axis Theorem, we shift this to the centroidal axes:

$$I_{xy} = I_{xy,0} - A \cdot x_c \cdot y_c \quad (84)$$

#### Normalized Product of Inertia

Following the normalization procedure ( $c = 1$ ), the dimensionless product of inertia is:

$$I_{xy,\text{norm}} := \underbrace{\left[ \frac{1}{2} \int_0^1 \xi(\eta_u^2 - \eta_l^2) d\xi \right]}_{I_{xy,0,\text{norm}}} - A_{\text{norm}} \cdot \xi_c \cdot \eta_c \quad (85)$$

This scales with the fourth power of the chord, consistent with the other moments of inertia:

$$I_{xy} = c^4 \cdot I_{xy,\text{norm}} \quad (86)$$

### 3.1.4 Principal Axes and Moments of Inertia

The principal axes are the set of orthogonal axes ( $u, v$ ) rotated by an angle  $\theta_p$  where the product of inertia vanishes ( $I_{uv} = 0$ ). This represents the orientation of maximum and minimum stiffness.

The rotation angle  $\theta_p$  to the principal axes is given by:

$$\tan(2\theta_p) = \frac{-2I_{xy}}{I_x - I_y} \quad (87)$$

The principal moments of inertia ( $I_1$  and  $I_2$ , typically corresponding to the stiffest and weakest axes respectively) are calculated as:

$$I_{1,2} = \frac{I_x + I_y}{2} \pm \sqrt{\left(\frac{I_x - I_y}{2}\right)^2 + I_{xy}^2} \quad (88)$$

Using these principal inertias allows for the decoupling of the bending equations into the natural coordinate system of the blade section.

However, SABEMMT code does *not* use principal axes of inertia, since they do not imply any computational benefit, and it is simpler to avoid the extra rotation of angle  $\theta_p$ .

## 3.2. Stress Estimation Model

The stress analysis relies on the "quasi-prismatic" assumption. Although the blade chord  $c(r)$  varies along the radius, the taper angle is assumed sufficiently small to apply standard beam theory locally at each blade station.

The total normal stress  $\sigma_z$  at a radial location  $r$  and cross-sectional point  $(x, y)$  is the superposition of the centrifugal tensile stress and the bending stresses.

### 3.2.1 Centrifugal Force

The centrifugal force  $F_{cf}(r)$  acting at a section  $r$  is the sum of the inertial forces of all blade mass elements outboard of that section (from  $r$  to the tip  $R$ ). The changing chord enters the integral via the area  $A(r)$ :

$$F_{cf}(r) = \int_r^R \rho \Omega^2 s A(s) ds \quad (89)$$

Where:

- $\rho$  is the material density.
- $\Omega$  is the rotational velocity (rad/s).
- $A(s) = c(s)^2 \cdot A_{\text{norm}}$  is the local cross-sectional area.

### 3.2.2 Bending Moments computation and rotation of moments to local axes

The existence of thrust ( $dT/dx$ ) and tangential force ( $dF_t/dx$ ) distributions generates bending moments in the propeller blades. These moments will be given by the force differentials ( $dT$  and  $dF_t$ ) applied at each section ( $r_k$ ), multiplied by their lever arm to the considered section ( $r_i$ ).

Computation of bending moments in rotor axes:

The bending moments in rotor axes are defined as:

$$M_T(r_i) = - \sum_{k=i}^N dT(r_k) (r_k - r_i) \quad (90)$$

$$M_{F_t}(r_i) = \sum_{k=i}^N dF_t(r_k) (r_k - r_i) \quad (91)$$

Where the negative sign in the expression of  $M_T$  indicates that, if we imagine the airfoil advancing to the left, positive thrust causes a moment in the negative direction of the  $x_{\text{airfoil}}$  axis (because  $x_{\text{airfoil}}$

points towards the trailing edge). See Figure 3.

#### Rotation of aerodynamic moments to local section axes:

It is important to note that we rotate the moments, not the forces. That is because if we rotated the force distribution, each  $dT$  and each  $dF_t$  would experience a different rotation due to the pitch angle changing throughout the blade. We wouldn't be able to add those rotated forces later to calculate moments, because they wouldn't all be in the same frame of reference.

Denoting the moment around  $x_{airfoil}$  axis as  $M_x$  and the moment around  $y_{airfoil}$  axis as  $M_y$ , since the airfoil is rotated an angle  $\theta$  clockwise with respect to the rotor plane, the rotation of moments is performed as follows:

$$\begin{aligned} \begin{bmatrix} M_x \\ M_y \end{bmatrix}_{\text{local}} &= \begin{bmatrix} \cos(-\theta) & \sin(-\theta) \\ -\sin(-\theta) & \cos(-\theta) \end{bmatrix} \begin{bmatrix} M_T \\ M_{F_t} \end{bmatrix} \\ &\Downarrow \quad \begin{aligned} \cos(-\theta) &= \cos \theta \\ \sin(-\theta) &= -\sin \theta \end{aligned} \\ \begin{bmatrix} M_x \\ M_y \end{bmatrix}_{\text{local}} &= \begin{bmatrix} \cos \theta & -\sin \theta \\ \sin \theta & \cos \theta \end{bmatrix} \begin{bmatrix} M_T \\ M_{F_t} \end{bmatrix} \end{aligned} \tag{92}$$

### 3.2.3 Total Normal Stress

Using the General Flexure Formula (which accounts for asymmetric bending where  $I_{xy} \neq 0$ ), the total stress at any point  $(x, y)$  on the airfoil section is:

$$\sigma_z(x, y) = \underbrace{\frac{F_{cf}}{A}}_{\text{Tension}} + \underbrace{\left( \frac{M_x I_y - M_y I_{xy}}{I_x I_y - I_{xy}^2} \right) y + \left( \frac{M_y I_x - M_x I_{xy}}{I_x I_y - I_{xy}^2} \right) x}_{\text{Bending}} \tag{93}$$

**Note:** All geometric properties  $(A, I_x, I_y, I_{xy})$  in this equation are the *local* values for the specific section at radius  $r$ , scaled by the local chord  $c(r)$ .

### 3.3. Calculation of Maximum Tension

Since the normal stress  $\sigma_z(x, y)$  is a linear function of the coordinates  $x$  and  $y$  (defining a planar stress field), the global maximum tension must occur at one of the points on the perimeter of the airfoil contour.

To locate this point efficiently we will only evaluate those perimeter points. We first condense the bending terms into two sensitivity coefficients,  $K_x$  and  $K_y$ , which represent the stress gradients in the chordwise and thickness directions respectively.

$$K_x = \frac{M_y I_x - M_x I_{xy}}{I_x I_y - I_{xy}^2}, \quad K_y = \frac{M_x I_y - M_y I_{xy}}{I_x I_y - I_{xy}^2} \tag{94}$$

The total stress equation simplifies to:

$$\sigma_z(x, y) = \sigma_{cf} + K_x \cdot x + K_y \cdot y \tag{95}$$

Where  $\sigma_{cf} = F_{cf}/A$  is the uniform centrifugal stress constant.

A visualization of the stress distribution at 3 different sections of the blade can be generated directly from the matlab code at: <https://github.com/miguel-frade/sabemmt>

#### 3.3.1 Algorithm for finding the point of maximum stress

Given the discrete set of  $N$  coordinates  $\{(x_i, y_i)\}$  defining the airfoil perimeter (scaled to the local chord):

1. Compute  $K_x$  and  $K_y$  for the current section using local loads and inertias.
2. Evaluate the bending component  $S_i = K_x x_i + K_y y_i$  for all  $i = 1 \dots N$ .

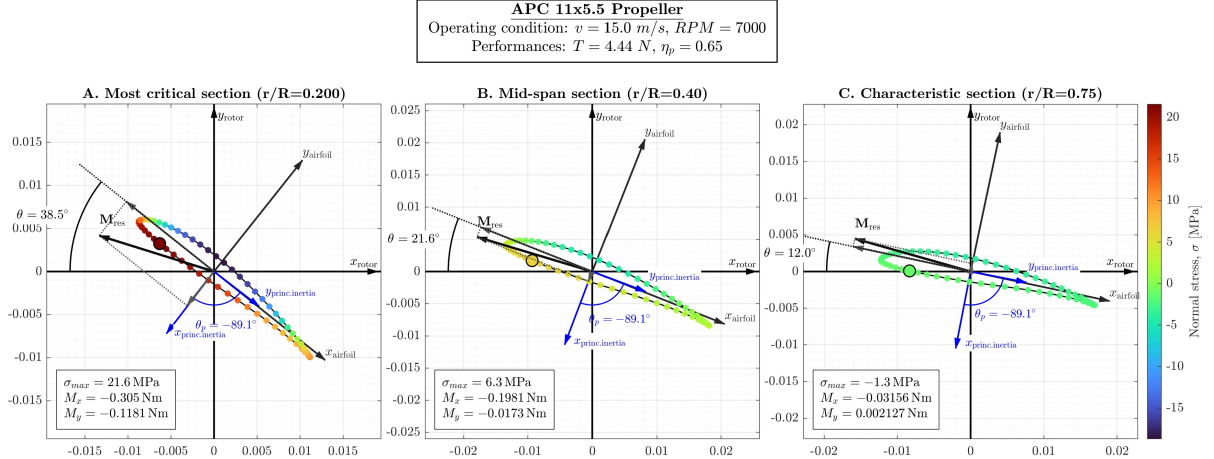


Figure 3: Airfoil stress distribution at three different sections of the blade. Automatically generated from: <https://github.com/miguel-frade/sabemmt>

3. Identify the index  $k$  such that  $S_k$  is maximized.
4. The maximum tension for the section is:

$$\sigma_{max} = \sigma_{cf} + S_k \quad (96)$$

This method reduces the search space to the airfoil boundary points ( $O(N)$  operations per section).

The maximum stress in the whole blade can be simply found as:

$$\sigma_{total,max,max} = \max(\sigma_{max}) \quad (97)$$

## 4. Possible simplification of the geometry for structural analysis (not implemented in SABEMMT code)

If the accuracy of structural analysis is not an important concern of the project, the geometry of the propeller sections can be simplified to rectangles rotated accordingly with the pitch distribution. This simplification permits a significant improvement in SABEMMT code performance.

Nonetheless, this simplification will, in fact, be very conservative (it will overestimate the stresses). While this approach improves safety in a design process, it may lead to overdimensioning of the structure.

Therefore, the previous structural model (section 3) is preferred for the SABEMMT model, and is the one implemented in the code.

### 4.1. Simplification of the geometry for structural calculations

The estimation of the stresses at each section of the blade is based on classical beam theory, which relates the force distributions on the blade with the stresses by knowing the area moments of inertia of the sections.

The possible simplification that can be used, models the geometry at each section as a rectangle of equal chord and area as the corresponding airfoil. That equivalent rectangle therefore has a thickness of:

$$\text{For a rectangle: } A = c t_{\text{equiv}} \rightarrow t_{\text{equiv}} = \frac{A}{c} \quad (98)$$

And since that thickness is smaller than the one of the original airfoil, the use of this equivalent rectangle is actually a conservative model.

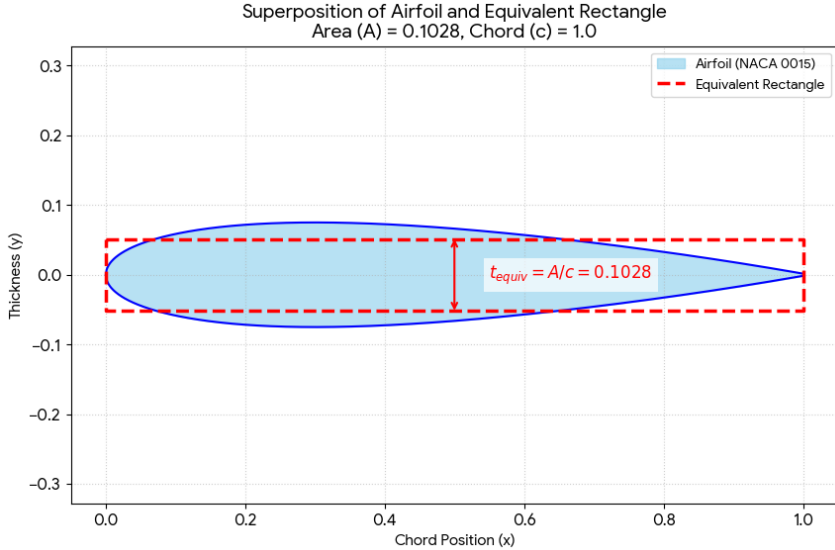


Figure 4: Rectangle of same Chord and Area.

We can easily compute the area moments of inertia for a  $c = 1$  rectangle and later just scale those inertias with  $c$  for any section of the blade, according to the following:

Normalized area and thickness (area and equivalent thickness of a  $c = 1$  airfoil) are defined as:

$$A_{\text{norm}} := \frac{A}{c^2} \quad (99)$$

$$t_{\text{equiv}} = \frac{A}{c} = \frac{A_{\text{norm}} c^2}{c} = A_{\text{norm}} c \quad \rightarrow \quad t_{\text{equiv},\text{norm}} := \frac{t_{\text{equiv}}}{c} = A_{\text{norm}} \quad (100)$$

And the area moments of inertia with respect to the local axis of the rectangle are simply:

$$I_x = \frac{ct_{\text{equiv}}^3}{12} = \frac{c(c t_{\text{equiv},\text{norm}})^3}{12} = \frac{c^4 t_{\text{equiv},\text{norm}}^3}{12} \quad \rightarrow \quad I_{x,\text{norm}} := \frac{I_x}{c^4} = \frac{t_{\text{equiv},\text{norm}}^3}{12} \quad (101)$$

$$I_y = \frac{t_{\text{equiv}} c^3}{12} = \frac{t_{\text{equiv},\text{norm}} c^4}{12} \quad \rightarrow \quad I_{y,\text{norm}} := \frac{I_y}{c^4} = \frac{t_{\text{equiv},\text{norm}}}{12} \quad (102)$$

#### 4.1.1 Scaling to real chord

The inertias computed for a  $c = 1$  rectangle can easily be scaled to any rectangle of chord  $c$  by doing:

$$I_x = c^4 \underbrace{\left( \frac{t_{\text{equiv},\text{norm}}^3}{12} \right)}_{I_{x,\text{norm}}} = c^4 \cdot I_{x,\text{norm}} \quad (103)$$

$$I_y = c^4 \underbrace{\left( \frac{t_{\text{equiv},\text{norm}}}{12} \right)}_{I_{y,\text{norm}}} = c^4 \cdot I_{y,\text{norm}} \quad (104)$$

The area (which is needed to compute the stress caused by centrifugal forces) can also be scaled to each section dimension by doing:

$$A = c^2 \cdot A_{\text{norm}} \quad (105)$$

## 4.2. Calculation of centrifugal force and centrifugal stresses

Centrifugal force acts in the radial direction due to the rotation of the blade with angular velocity  $\Omega$  and material density  $\rho_{\text{mat}}$ .

### 4.2.1 Accumulated centrifugal force

For each section  $r$ :

$$F_{\text{cf}}(r) = \int_r^R \rho_{\text{mat}} \Omega^2 A(s) s ds \quad (106)$$

### 4.2.2 Centrifugal stresses

Dividing by the section area:

$$\sigma_{\text{cf}}(r) = \frac{F_{\text{cf}}(r)}{A(r)} \quad (107)$$

## 4.3. Bending stresses

Being conservative, we can just consider the maximum stress caused by  $M_x$  and the maximum stress caused by  $M_y$  in the rectangle as absolute values:

$$\sigma_{\text{bend,max},M_x} = \left| \frac{M_x (t_{\text{equiv}}/2)}{I_x} \right| \quad (108)$$

$$\sigma_{\text{bend,max},M_y} = \left| \frac{M_y (c/2)}{I_y} \right| \quad (109)$$

This simplification of only computing the stress at one point of each section instead of  $N$  points is what makes this approach of using rectangles faster, but much less accurate than the approach detailed in section 3.

## 4.4. Total stress

Combining bending and centrifugal stresses, we obtain the total tensile stress at the most critical point of a particular section:

$$\sigma_{\text{total,max}}(r) = \sigma_{\text{bend,max},M_x}(r) + \sigma_{\text{bend,max},M_y}(r) + \sigma_{\text{cf}}(r) \quad (110)$$

And the maximum stress in the whole blade will be:

$$\sigma_{\text{total,max,max}} = \max(\sigma_{\text{bend,max},M_x}(r) + \sigma_{\text{bend,max},M_y}(r) + \sigma_{\text{cf}}(r)) \quad (111)$$

## References

- Cuerva Tejero, Álvaro, J. L. Espino Granado, et al. (2012). *Teoría de los helicópteros*. 2nd ed. Madrid: Garceta. ISBN: 978-84-1545-221-8 (cit. on p. 5).
- Cuerva Tejero, Álvaro, Ángel P. Sanz Andrés, et al. (2006). “An engineering modification of the blade element momentum equation for vertical descent: an autorotation case study”. In: *Aerospace Science and Technology* (cit. on pp. 1, 5).
- McCormick, Barnes W. (1979). *Aerodynamics, Aeronautics, and Flight Mechanics*. New York: John Wiley & Sons. ISBN: 0-471-03032-5 (cit. on p. 9).